Characterization of a Novel Energy Efficient Atomizer Employing Countercurrent Shear

A. Hoxie[1*], E. Johnson[1], V. Srinivasan[2], P. Strykowski[2]
[1]University of Minnesota Duluth, USA
[2]University of Minnesota Twin Cities, USA

Abstract

The ability to atomize viscous liquids in an energy-efficient manner would enable significant cost-savings in combustion systems, potentially through the adoption of alternative fuels such as heavier grades or biomass-based oils. Conventional air-assist or air-blast atomizers rely on high levels of mean shear between the liquid stream and the air stream, and exhibit diminishing returns in performance as the kinetic energy of the air-stream is increased, leading to poor energy efficiency. We present a novel air-assist atomizer, which employs a counterflow configuration between the liquid and air streams, generating high levels of turbulent kinetic energy production and improving atomization. Experiments were performed with fluids of varying viscosity, from water to fluids with viscosities 40-times that of water and for flowrates from 2.3 g/s up to 4.2 g/s. The novel atomizer, named the counterflow nozzle, is an internal mixing nozzle and was compared to commercially available internal mixing air-assist nozzles designed to operate at similar flow rates. The counterflow nozzle consistently developed similar Sauter Mean Diameters (SMDs) as the commercial nozzle at all flow rates tested for water, but with the advantage of using only half the air mass flow. As the viscosity of the fluids tested increased, the counterflow nozzle developed sprays with smaller SMDs and a tighter droplet distribution as compared with the commercial nozzle, but again at half the amount of air flow rate. The significant improvement in atomization is explained on the basis of linear stability analysis of the counterflowing streams inside the nozzle.

Keywords: Spray, atomization, measurement, drop size, imaging diagnostics

Introduction

The transformation of a liquid from a continuous bulk phase to a dispersed phase with small droplets is a requirement in several industrial situations such as pesticide application, pharmaceutical and food processing, painting, and combustion. Depending on the application, the energy required for overcoming the cohesive effects of surface tension and viscosity may be supplied through several means, such as mechanical, ultrasonic or electrostatic forcing. In pressure atomizers, liquid is injected at high pressure into a quiescent ambient, and the high relative velocity between the liquid and the surrounding gas is responsible for the growth of instabilities at the liquid-gas interface. The precise mechanism of breakdown depends on the global geometry (liquid jet vs sheet); different breakup mechanisms dominate over a range of the relevant non-dimensional numbers (liquid jet Reynolds number, Weber number based on gas velocity) [1]. At low We, the dominant wavelengths of instabilities are of the order of the jet diameter, while shorter interfacial modes dominate as We increases, leading to atomization at high We. In pneumatic atomizers such as air-assist and air-blast configurations, the kinetic energy of a high-speed stream of gas is transferred to the liquid, which is typically in the form of a jet or sheet, causing disintegration of the liquid into fragments [2-3]. While the precise geometry for introducing the gas and liquid streams through the nozzle may vary, the common feature of external mixing nozzles is that the gas and liquid flows begin to interact as they leave their respective discharge orifices into the ambient. The breakdown process can be described by a sequence of instabilities, starting with primary atomization in which the jet develops shear instabilities at the interface that are chiefly determined by the thickness of the gas boundary layer [4-5], but may also depend on the vorticity in the liquid [6]. These instabilities lead to the formation of membranes and ligaments that peel off from the jet, developing instabilities of their own and break up into large drops. Finally, large drops undergo distortion and breakup due to aerodynamic forces, a process known as secondary atomization [6]. In addition to the liquid Reynolds number and Ohnesorge number, additional parameters based on relative values of velocity such as the relative Reynolds and Weber numbers, mass fluxes and momentum ratios become important [6-7].

While coaxial streams of liquid and air in external mixing nozzles represent a canonical case suitable for laboratory study, no similar situation can be envisaged for internal mixing nozzles. In such nozzles, liquid and air streams are introduced into a mixing chamber, where the liquid is typically formed into a thin film through impingement on to a deflector plate. The film undergoes primary atomization into large ligaments which emerge

from the nozzle and break up further under the action of the gas stream into smaller drops. Effervescent atomization [8], in which gas bubbles introduced into a mixing chamber rapidly expand and shatter the liquid interface, is another example of an internal mixing design. Understanding of the basic fluid mechanics in these confined geometries has been hindered by the complex multiphase flow and irregular interface, along with the lack of optical access.

All external mixing designs, as well as some internal mixing nozzles exploit mean shear to overcome the intermolecular forces tending to prevent liquid surface deformation. While liquid-gas interfaces exhibit natural instabilities that can lead to single-droplet formation, high *mean stress* is often necessary to accelerate and control the practical atomization process, particularly for high viscosity liquids. High mean stress also leads to elevated turbulent levels that accelerate the atomization process through kinetic energy fluctuations over a range of physical scales conducive to droplet breakup.

Countercurrent shear was first systematically examined in the laboratory in the late 1980's, following theoretical studies suggesting the potential for exceptionally high turbulent kinetic energy production associated with the unique absolute instability of the base flow field [9-10]. The key feature of countercurrent shear can only be realized in practical applications if the mean velocity travels in opposite directions in the reference frame of the device itself. This unique mean velocity field creates very high *turbulent stress*, which together with the inherent mean stress is capable of atomizing at substantially lower air input and thereby air energy delivery requirements. Forliti et al [11] measured enhancements of up to 75% in turbulent stress levels when the counterflow velocity in a dump combustor was increased to 30% of the main flow. Counterflow designs have been successfully demonstrated to significantly enhance shear and provide control in applications such as thrust vectoring [12] and increased heat release in combustion [13]. The current study represents the first known effort towards translate the well-established destabilizing influence of counterflow in single-phase flows to a two-phase situation.

The nozzle configuration shown in figure 1 illustrates how this concept is being used at the University of Minnesota to efficiently atomize viscous liquids. The liquid stream is introduced through a central tube; gas assist is provided in a secondary passageway, which is turned essentially 180° prior to being introduced largely about the periphery of the liquid. Choosing appropriate dimensions for the annular region of reversed flow by making it long relative to the annular gap width, one can ensure the development of well-defined velocity profiles for the reversed gas flow before it encounters and shears the liquid flow.

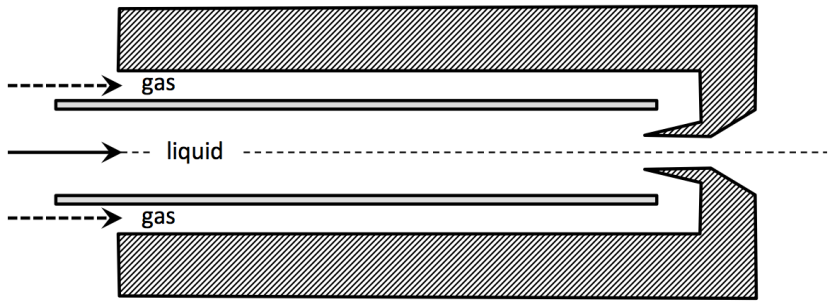

Figure 1. Schematic diagram showing the reversed flow direction of atomizing gas near the nozzle exit in a counterflow nozzle.

Initial measurements of the CF Nozzle operated with water-air and glycol-air show the technology is able to produce sprays of comparable quality to existing nozzles, but at energy requirements of half to less than half of current technology.

Experimental Methods

Figure 2 shows a sketch of the near-tip geometry of two counterflow nozzles recently developed at UMN. The spray exits to the ambient through a hypodermic needle of inner diameter d_0 and outer diameter d_1. The axial insertion of this needle upstream into a liquid supply line of inner diameter d_2 is denoted by a distance L. Air flows through the annular space formed between the liquid supply tube and an outer housing. The axial overlap of length L and annular gap $(d_1-d_0)/2$ between the needle and the liquid supply line causes the air flow to reverse its direction

and also controls the velocity magnitude. Table 1 shows the values used for these length scales in the two nozzles tested.

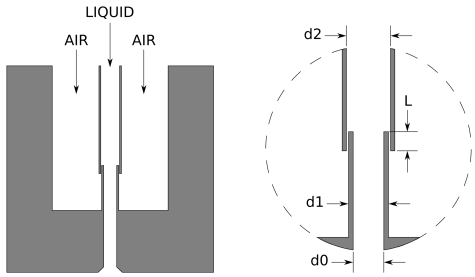

Figure 2: Sketch of nozzle geometry showing relevant dimensional parameters

	d_0 (mm)	d_1 (mm)	d_2 (mm)	L (mm)
CF4	1.6	2.1	2.3	1
CF2	1.96	1.45	1.26	1

Table 1. Values of dimensions used in CF4 and CF2 nozzles

Experiments conducted at the UMN Duluth Counterflow Shear Control Laboratory explored the atomization quality of the CF4 and CF2 nozzles at water flow rates of 4.2 g/s and 2.3g/s respectively, across a range of air pressures. The effect of liquid viscosity was also probed, atomizing 2.2 g/s of propylene glycol with the CF2 nozzle. As a point of comparison, commercial air-assist internal mixing nozzles rated for the same liquid flow rates were tested alongside the counterflow nozzles.

Figure 3 shows the test setup. Main air supply pressure was manipulated using a typical filter-regulator combo with sintered bronze 40-micron filter. In conjunction with a hand-operated ball valve, a digital Cole Parmer gas mass flowmeter (laminar flow element type) controlled and monitored air flow rates with +/- 1% accuracy. Liquid at the tested flow rates was supplied directly by a Micropump suction shoe pump head with digital 60–3600 RPM Cole Parmer gear drive. For glycol the indicated pump flow rate was found to be correct, but in the case of water a rotameter (variable area flowmeter) measured actual water flow rate with +/- 2% repeatability. A simple Bourdon gauge measured liquid pressure at the nozzle inlet.

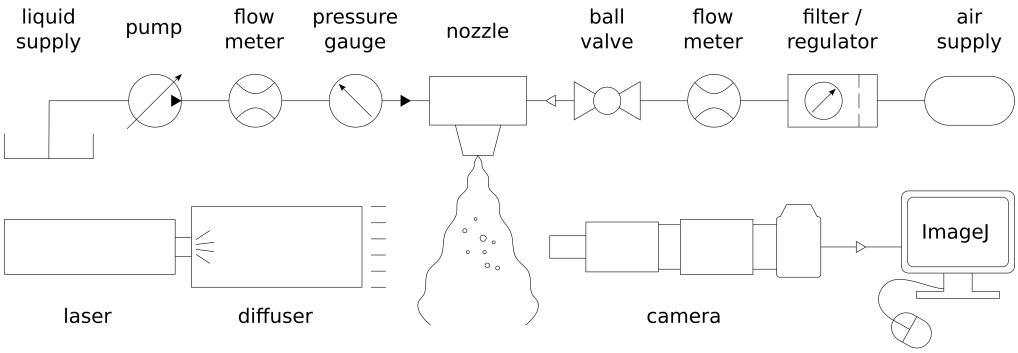

Figure 3: Shadowgraphy test setup for air-assist atomization.

Drops were imaged using standard shadowgraphic techniques utilizing a pulsed laser as a light source to provide a diffuse background. A Quantel EverGreen Nd:YAG laser provided pulsed 532 nm lighting at 10 Hz with <10

ns pulse width and energy of 145 mJ per pulse. The beam was manipulated into a uniform backlight for the spray with the use of two –25 mm cylindrical lenses followed by a diffuser. Images were captured with a Nikon D90 SLR camera, fitted with a 2x Nikon teleconverter in addition to an Infinity DistaMax K2 with CF-4 Objective and 1.66x CF Tube. This arrangement resulted in a magnification that yielded 3 image pixels per micron, with a 1 x 0.67 mm field of view. To allow two-dimensional radial placement of the image window in the spray, the camera and lens were bolted to an optical rail and two micrometer-adjust stages. As an arbitrary single point of comparison for spray quality, all droplet data was collected at a downstream distance of 15 mm from the nozzle outlet on the cylindrical axis. At this distance, the spray had expanded enough to avoid droplet overlap in images while also facilitating laser penetration of the spray cloud.

Adjusting the DSLR exposure time to ensure a single laser pulse per image, 300–500 images were captured for each spray condition. Depending on spray quality, 20,000–100,000 droplets were processed in each test. Convergence analysis of the SMD statistic suggested a 20,000 droplet minimum per test. ImageJ particle analysis libraries were used for image analysis on all droplets down to 5 microns in diameter. Images were saved as 8-bit JPG images, and a threshold value was applied to isolate drop shapes, from which droplet areas and effective diameters were calculated. No attempt to correct depth of field bias or other slight effects as proposed by researchers [14-15]. These corrections are known to be negligible for the small droplet sizes presented here. Values of SMD numbers reported here would be expected to decrease slightly at best with the addition of such correction models or treatment of droplets below 5 microns.

Results and Discussion

Figure 4 shows a high-speed image of the flow, taken at an exposure time of 1 μs. It is observed that the spray emerges from the nozzle exit orifice in the form of a solid cone. Intriguingly, unlike other internal mixing nozzles which usually display fluid ligaments that quickly disintegrate into droplets, either through the action of aerodynamic forces or bubble expansion, the image suggests that the droplets are formed upstream of the nozzle exit and are propelled out by the air flow. This would suggest an atomization mechanism that is different from the processes occurring in internal mixing nozzles such as Y-Jet designs [16], effervescent atomizers [8] or flow-blurring atomizers [17-18]. A distinctive feature of the flow inside the nozzle is the potential for the formation of extremely thin shear layers on the liquid and air streams, which may lead to interfacial instabilities of very short wavelength. Further studies are planned to elucidate this process.

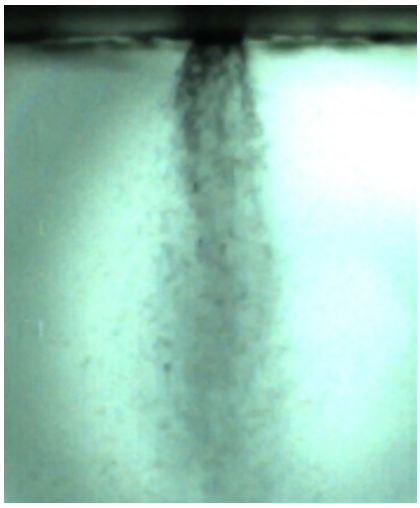

Figure 4. High speed visualization of spray emerging from a CF4 nozzle.

Baseline Experiments

Baseline experiments were conducted to compare the performance of the counterflow nozzle with off-the-shelf commercial air-assist nozzles. Tests were carried out with water at a volumetric flow rate of 2.3 g/s. The counterflow nozzle- herein labeled CF2, was compared to a commercial nozzle sized for the corresponding flow rate—labelled COM2. Figure 5 shows the cumulative volume fraction as a function of droplet diameter for a fixed inlet pressure of 414 kPa.

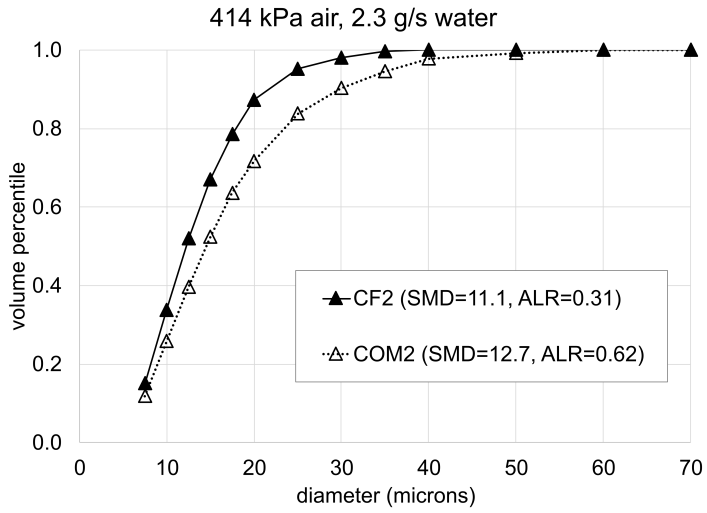

Figure 5: Baseline comparison of the Commercial Nozzle and Counterflow Nozzle CF2 at a water flow rate of 2.3 g/s.

It can be observed that the droplet diameter distribution of the spray exiting the counterflow nozzle is similar to that from the commercial nozzle. The Sauter Mean Diameter (SMD) for the CF2 and COM2 nozzles are 11.1 μm and 12.7 μm respectively. The ability to produce small SMDs with a tight distribution ratio is closely linked to the amount of compressed air in the spraying system and its delivery pressure. For the flow given in fig. 5 the air-to-liquid ratio (ALR) based on mass flow rate for CF2 and COM2 were 0.31 and 0.62, respectively. This means the counterflow nozzle was able to produce a nearly identical spray as compared to the commercial nozzle but with half the air mass flow rate. For this comparison at constant inlet pressure of air, which fixes the enthalpy difference, the counterflow nozzle exhibits a 50% reduction in energy to produce a similar spray.

Role of Air Supply Pressure

The Counterflow nozzle was compared to an off-the-shelf commercial nozzle at various pressures for a fixed water flow rate of 4.2 g/s. Figure 6 provides cumulative volume percentile vs droplet diameter for air inlet pressures (gauge) of 386 kPa, 441 kPa, 483 kPa and 552 kPa. The spray distributions from the two nozzles are quite close, with the diameter distribution from the CF4 nozzle gradually shifting towards the COM4 distribution as pressure is increased. Values of SMD and ALR are provided on each graph. The greatest difference in SMD between the two nozzles occurs at the lowest pressure of 386 kPa. The SMD is 13% larger than the commercial nozzle at the lowest pressure, however for the other test cases the SMD from the counterflow nozzle is within 8% of the COM4 value.

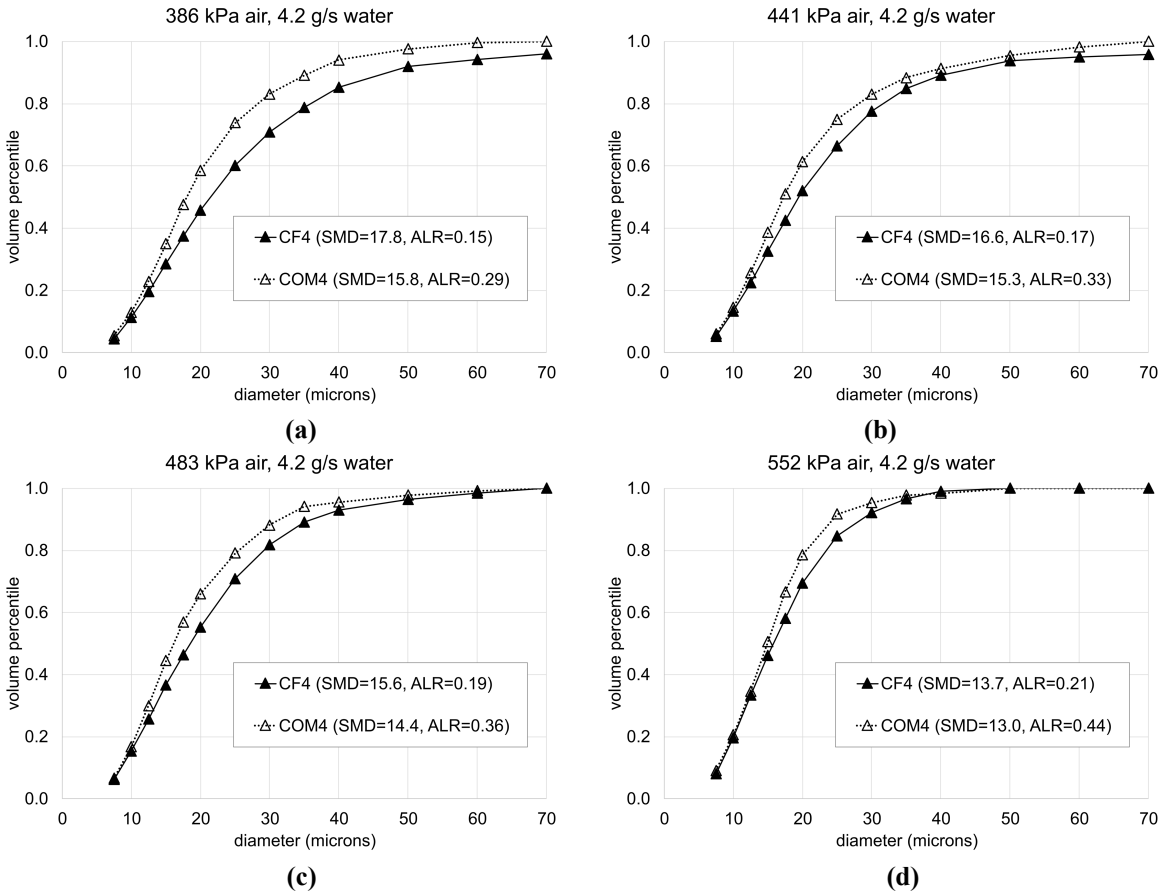

Figure 6: Cumulative volume fraction distribution for the CF4 and COM4 nozzles at a flow rate of 4.2 g/s for various air inlet pressures: a) 386 kPa, b) 441 kPa, c) 483 kPa, d) 552 kPa.

Figure 7 provides a comparison of ALR and compressor energy required to provide the atomizing air to the nozzle for each of the pressures tested for a liquid flow rate of 4.2 g/s. Figure (a) indicates that it is possible to attain SMD values of 10-20 mm with low values of ALR relative to the ALR required by the COM4 nozzle. Interestingly, the CF4 nozzle is also more sensitive to changes in absolute levels of ALR, the SMD drops by 35% for a change of 0.1 in ALR. By comparison, the sensitivity of SMD to ALR is weaker for the COM4 nozzle. At the highest pressures tested, the two nozzles produce similar values of SMD (COM4: 13.0 mm, CF4: 13.7 mm). However, the ALR values required to produce these sprays are 0.21 (CF4) and 0.44 (COM4), translating to a 51% reduction in pumping energy. Energy consumption for all pressures tested are shown in figure 7(b) and indicate that the greatest performance benefit of the CF4 nozzle lies at higher pressures, where substantially lower flow rates are required to produce the same value of SMD compared to the COM4 nozzle.

The data presented thus far suggests that the counterflow nozzle can develop comparable sprays but at a significant reduction in energy. To ensure that the sprays developed by both nozzles are truly similar the Relative Span Factor (RSF) and DV90 were plotted and are provided in figure 8. RSF is equal to (DV90 - DV10) / DV50. It is a measure of spray uniformity, if RSF=0, all droplets same size. DV90 = 90th volume percentile, meaning 90% of spray volume is observed in droplets of diameter less than DV90. Some deviation is seen for the counteflow nozzle at the lowest pressure, however as the pressures increase, the counterflow nozzle performs very similar to the commercial nozzle. At the highest pressure of 552 kPa where the greatest energy reduction is seen, DV90 is 29 microns for CF4 and 23.8 microns for COM4.

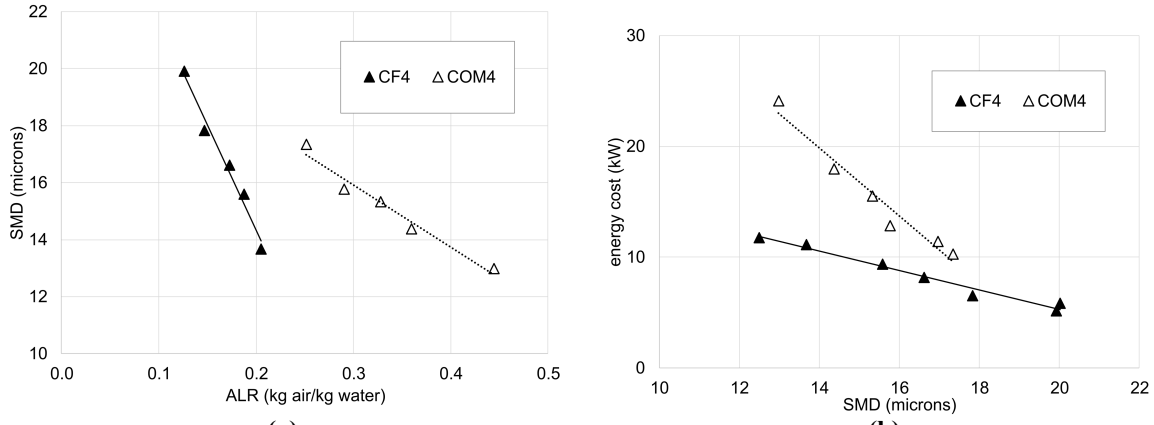

(a) (b)

Figure 7: a) SMD vs ALR for water at 4.2 g/s, b) energy required to supply compressed air as a function of SMD for water flowing at 4.2 g/s.

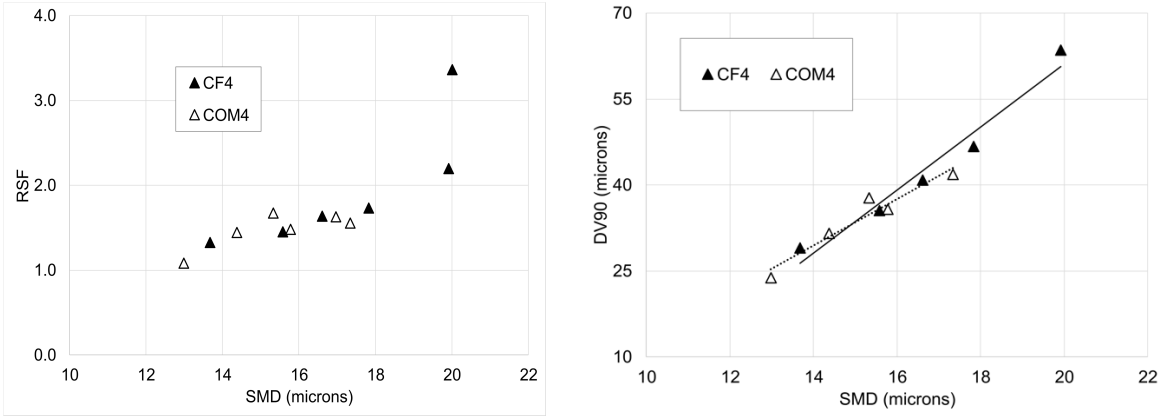

(a) (b)

Figure 8 (a) Relative Span Factor for CF4 and COM 4 nozzles at various inlet pressures, (b) DV90

Role of Viscosity

The ability of the counterflow nozzle to efficiently atomize fluids of higher viscosity was also explored and compared to the commercial nozzle. Propylene glycol was chosen for comparison because it is 40 times more viscous than water, readily available, and water soluble. Spray distributions were compared for a glycol mass flow rate of 2.2 g/s with an air supply pressure of 414 kPa. Figure 9 provides the cumulative volume percentile versus droplet diameter size in microns for the CF2 and COM2 nozzles. The CF2 counterflow nozzle produces a narrower droplet distribution over the commercial nozzle. Similar to the water-air experiments, the ALR for CF2 was 50% less than COM2, however the SMD for CF2 was substantially lower than the commercial nozzle. Unlike the water/air systems, however, where the reduction in ALR was achieved for similar values of SMD, here the reduction in ALR is accompanied by a substantial reduction in SMD. The SMD for the CF2 was 16.1 μm and 25.6 μm for COM2.

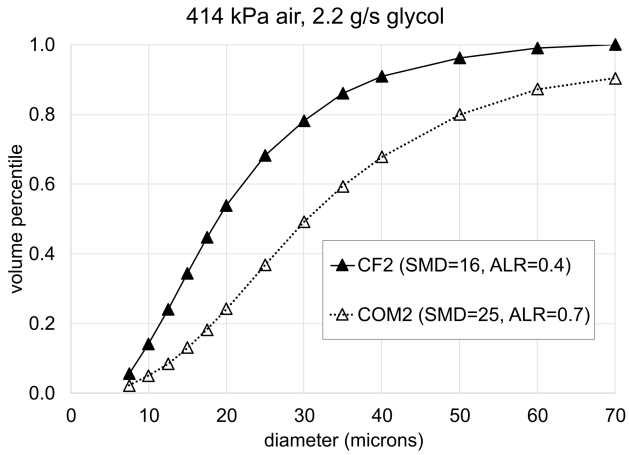

Figure 9. Cumulative volume fraction for propylene glycol sprayed at 2.2 g/s and an air inlet pressure of 414 kPa.

Summary and Conclusions

The counterflow nozzle exhibits features shared by all internal mixing designs compared to external mixing designs; these include lower atomizing air requirements and relatively lower sensitivity to liquid viscosity. However, these features seem to be significantly stronger in the counterflow design. The most significant outcome of this study is that even for large flow rates, SMD values remain at or less than 20 microns, despite using ALR values less than 0.2. The high sensitivity of the SMD to ALR shown in fig 7a suggests that much smaller values of SMD may be attained without significant increases in ALR, though this remains to be verified. The overall effect of this behavior is to yield a significantly increased efficiency, defined in terms of the surface area generated for a given power input towards air compression. Efficiency over a commercially available nozzle is increased by nearly 100%. For reasons that are not currently established, this performance trend is shown to increase as the liquid viscosity increases. The mechanism responsible for this behavior remains to be studied.

References

[1] S. P. Lin and R. D. Reitz, "Drop and Spray Formation From a Liquid Jet," *Annu. Rev. Fluid Mech.*, vol. 30, no. 1, pp. 85–105, 1998.

[2] M. Gorokhovski and M. Herrmann, "Modeling Primary Atomization," *Annu. Rev. Fluid Mech.*, vol. 40, no. 1, pp. 343–366, 2008.

[3] J. C. Lasheras and E. J. Hopfinger, "Liquid Jet Instability and Atomization in a Coaxial Gas Stream," *Annu. Rev. Fluid Mech.*, vol. 32, pp. 275–308, 2000.

[4] A. Lozano and F. Barreras, "Longitudinal instabilities in an air-blasted liquid sheet," *J. Fluid Mech.*, vol. 437, pp. 143–173, 2001.

[5] T. Funada, D. D. Joseph, and S. Yamashita, "Stability of a liquid jet into incompressible gases and liquids," *Int. J. Multiph. Flow*, vol. 30, no. 11, pp. 1279–1310, 2004.

[6] D. R. Guildenbecher, C. López-Rivera, and P. E. Sojka, "Secondary atomization," *Exp. Fluids*, vol. 46, no. 3, pp. 371–402, 2009.

[7] J. C. Lasheras, E. Villermaux, and E. J. Hopfinger, "Break-up and atomization of a round water jet by a high-speed annular air jet," *J. Fluid Mech.*, vol. 357, no. 1998, pp. 351–379, 1998.

[8] S. D. Sovani, P. E. Sojka, and A. H. Lefebvre, "Effervescent atomization," *Progress in Energy and Combustion Science*, vol. 27, no. 4. pp. 483–521, 2001.

[9] P. J. Strykowski and D. L. Niccum, "The stability of countercurrent mixing layers in circular jets," *J. Fluid Mech.*, vol. 227, pp. 309–343, Apr. 1991.

[10] P. A. Monkewitz, P. Huerre, and J.-M. Chomaz, "Global linear stability analysis of weakly non-parallel shear flows," *J. Fluid Mech.*, vol. 251, no. 1, p. 1, Apr. 1993.

[11] D. Forliti and P. Strykowski, "Controlling turbulence in a rearward-facing step combustor using countercurrent shear," *J. Fluids Eng.*, vol. 127, no. 3, pp. 438–448, 2005.

[12] P. Strykowski, A. Krothapalli, and D. Forliti, "Counterflow thrust vectoring of supersonic jets," *AIAA J.*, vol. 34, no. 11, pp. 2306–2314, Nov. 1996.

[13] A. A. Behrens and P. J. Strykowski, "Controlling Volumetric Heat Release Rates in a Dump Combustor Using Countercurrent Shear," *AIAA J.*, vol. 45, no. 6, pp. 1317–1323, 2007.

[14] K. S. Kim and S.-S. Kim, "Drop sizing and depth-of-field correction in TV imaging," *At. Sprays*, vol. 4, no. 1, 1994.

[15] K. U. Koh, J. Y. Kim, and S. Y. Lee, "Determination of in-focus criteria and depth of field in image processing of spray particles," *At. Sprays*, vol. 11, no. 4, 2001.

[16] M. Sargeant, "Blast atomizer developments in the central electricity generating board," in *Proceeding of the Second International Conference on Liquid Atomization and Spray Systems*, 1982, pp. 131–135.

[17] A. M. Gañán-Calvo, "Enhanced liquid atomization: From flow-focusing to flow-blurring," *Appl. Phys. Lett.*, vol. 86, no. 21, pp. 1–3, 2005.

[18] B. M. Simmons and A. K. Agrawal, "Spray Characteristics of a Flow-Blurring Atomizer," *At. Sprays*, vol. 20, no. 9, pp. 821–835, 2010.